



Contents lists available at ScienceDirect

Bioorganic & Medicinal Chemistry Letters

journal homepage: www.elsevier.com/locate/bmcl

Synthesis of potent chemical inhibitors of dynamin GTPase

Suho Lee^{a,b,c,†}, Kwan-Young Jung^{a,†}, Joohyun Park^{b,c}, Joong-Heui Cho^a, Yong-Chul Kim^a, Sunghoe Chang^{b,c,*}^a Department of Life Science, Gwangju Institute of Science and Technology, Gwangju 500-712, South Korea^b Department of Physiology and Biomedical Sciences, Seoul National University College of Medicine, Seoul 110-799, South Korea^c Neuroscience Research Institute, Medical Research Center, Seoul National University College of Medicine, Seoul 110-799, South Korea

ARTICLE INFO

Article history:

Received 27 February 2010

Revised 7 June 2010

Accepted 17 June 2010

Available online 22 June 2010

Keywords:

Dyasore

Dynamin

GTPase

Clathrin

Endocytosis

Transferrin

ABSTRACT

Dynamin is a key regulatory protein in clathrin mediated endocytosis. Compared to genetic or immunological tools, small chemical dynamin inhibitors such as dynasore have the potential to study the dynamic nature of endocytic events in cells. Dynasore inhibits dynamin GTPase activity and transferrin uptake at $IC_{50} \sim 15 \mu M$ but use in some biological applications requires more potent inhibitor than dynasore. Here, we chemically modified the side chains of dynasore and found that two derivatives, DD-6 and DD-11 more potently inhibited transferrin uptake (IC_{50} : $4.00 \mu M$ for DD-6, $2.63 \mu M$ for DD-11) and dynamin GTPase activity (IC_{50} : $5.1 \mu M$ for DD-6, $3.6 \mu M$ for DD-11) than dynasore. The effect was reversible and they were washed more rapidly out than dynasore. TIRF microscopy showed that they stabilize the clathrin coats on the membrane. Our results indicated that new dynasore derivatives are more potent inhibitor of dynamin, displaying promise as leads for the development of more effective analogues for broader biological applications.

© 2010 Elsevier Ltd. All rights reserved.

Dynamin is essential for clathrin-coated vesicle formation in endocytosis, at the trans Golgi network, as well as for the fission of caveolae.^{1–6} It consists of a GTPase module, a pleckstrin-homology (PH) domain, a GTPase effector domain (GED), and a proline/arginine-rich C-terminal segment (PRD). Dynamin works as a mechanochemical enzyme that induces conformational change through GTP hydrolysis which leads to constriction and scission of neck of a budding pit.⁷ A few endocytosis inhibitors such as chlorpromazine, concanavalin A, phenylarsine oxide, dansylcadaverine, had been suggested but had suffered from poor specificity and no specific biological target.^{8–12} Targeting the GTPase activity of dynamin has been attractive candidate for an endocytosis inhibitor, and a few small molecule inhibitors have been developed. Recently, Macia et al. screened 16,000 compounds to find one with the ability to block the GTPase activity of dynamin and have identified dynasore ($C_{18}H_{14}N_2O_4$, molecular weight 322.31 g/mol), that interferes in vitro with the GTPase activity of dynamin1, dynamin2, and Drp1, the mitochondrial dynamin, but not of other small GTPases.¹³

Abbreviations: EtOH, ethanol; DMAP, 4-dimethylaminopyridine; DCM, dichloromethane; DMSO, dimethylsulfoxide; HCl, hydrochloric acid; $CHCl_3$, chloroform; TEA, triethylamine; Bop-Cl, bis(2-oxo-3-oxazolidinyl)phosphonic chloride; EDCl, 1-ethyl-3-(3-dimethylaminopropyl)carbodiimide; Na_2SO_4 , sodium sulfate; TIRF, total internal reflection fluorescence.

* Corresponding author. Address: Department of Physiology and Biomedical Sciences, Seoul National University College of Medicine, #309 Biomedical Science Building, 28 Yeongeon-dong Jongno-gu, Seoul 110-799, South Korea.

† These authors contributed equally.

Dyasore reversibly inhibits the GTPase activity of dynamin1 or dynamin2 at the plasma membrane in a dose-dependent manner with IC_{50} of $\sim 15 \mu M$. At $80 \mu M$, dynasore also inhibits the enzymatic activity of the mitochondrial dynamin Drp1. Dynasore blocks internalization of transferrin, LDL, and cholera toxin.^{13,14} There has been, however, concern about the instability of dynasore, and moreover, the working concentration for dynasore ($\sim 80 \mu M/0.2\%$ DMSO final) is not suitable for some sensitive experiments such as electrophysiological measurement in neuron, thereby asking for more potent inhibitor than dynasore.

Dyasore (DD-4) was synthesized as previously described.¹⁴ Then, we designed a series of dynasore derivative compounds, focusing synthetic approach of the corresponding amide analogues, 2-naphthohydrazides and 2-naphthoamides which resulted in potent and stable inhibitory effect. *N*'-substituted 2-naphthohydrazide (DD-4–11), *N*'-substituted 2-naphthoamide (DD-12–19), and Bop-2-naphthoate (DD-20) were synthesized in good overall yields by solution phase methods, as shown in Figure 1. Starting materials of these reactions were commercially available 3-hydroxy-2-naphthoic acid ($R_1 = OH$) and 2-naphthoic acid ($R_1 = H$). The carboxylic acid group of starting material (DD-1) was coupled with methanol in well established Fischer esterification method to give ester group containing compound (DD-2). Ester group of 2-naphthoate (DD-2) was easily substituted by treatment with hydrazine monohydrate in anhydrous ethanol at $20^\circ C$ for 24 h to furnish the desired hydrazide containing compound (3). Eight kinds of *N*'-substituted 2-naphthohydrazide (DD-4–11) compounds were synthesized by reductive amination with 2-naphthohydrazide (3)

and various benzaldehyde.¹⁵ For the synthesis of the N-substituted 2-naphthoamide (DD-12–19), the starting material (DD-1) was activated with EDCI reagent, which was easily attacked by amine compound in the described conditions. The amide bond step to compound DD-12–19 proceeded in satisfactory yields by following a typical EDCI/DMAP coupling protocol.¹⁶ In order to synthesis the Bop-2-naphthoate (DD-20), 2-naphthoic acid was dissolved in DCM and triethylamine was added to activate the carboxylic acid and then Bop-Cl was added to the reaction bottle (Fig. 1 and Table 1; Details of syntheses containing NMR and Mass data are described in Supplementary data).¹⁷

To test the fast-acting inhibitory activity of new analogues, we performed transferrin uptake assay without pre-treatment.¹⁸ We treated COS-7 cells with TexasRed–transferrin for 10 min at 37 °C in the presence or absence of 80 μ M dynasore or its analogues. In control cells, TexasRed–transferrin rapidly internalizes and accumulates in peripheral early endosomes (Fig. 2).¹⁹ Treatment with 80 μ M dynasore efficiently blocked transferrin uptake as previously reported. The substitution of hydroxyl group of 3-position on the naphthyl ring in dynasore to hydrogen (DD-6) and introduc-

tion of hydroxyl group at 3' and methoxy group at 4' on phenyl ring (DD-11) also showed comparable inhibitory effect on transferrin uptake to dynasore. Introduction of chlorine atoms at 4' and 5' position on phenyl ring (DD-5) completely lost the inhibitory effect on dynamin GTPase. Dimethyl substituted compounds at 4' and 5' position of phenyl ring also showed the lack of inhibition (Fig. 2).

We tested the dose-dependency of DD-6 and DD-11 and determined the median inhibition concentration (IC₅₀) of two analogues on transferrin uptake. Dynasore inhibits transferrin uptake in a dose-dependent manner with an IC₅₀ of \sim 15 μ M which is consistent with the previously reported value. The inhibition of transferrin uptake by DD-6 and DD-11 is also dose-dependent and has an IC₅₀ of \sim 4 μ M and \sim 2.6 μ M, respectively, suggesting that DD-6 and DD-11 are more potent inhibitor of transferrin uptake than dynasore (Fig. 3a–c).

We next tested whether new analogues inhibit dynamin GTPase activity *in vitro*.²⁰ Dynasore inhibits the GTPase activity of full-length dynamin1 stimulated by self-association (by exposure to low salt) in a dose-dependent manner with a median inhibition concentration (IC₅₀) of 10.8 μ M. DD-6 and DD-11 also inhibit dyn-

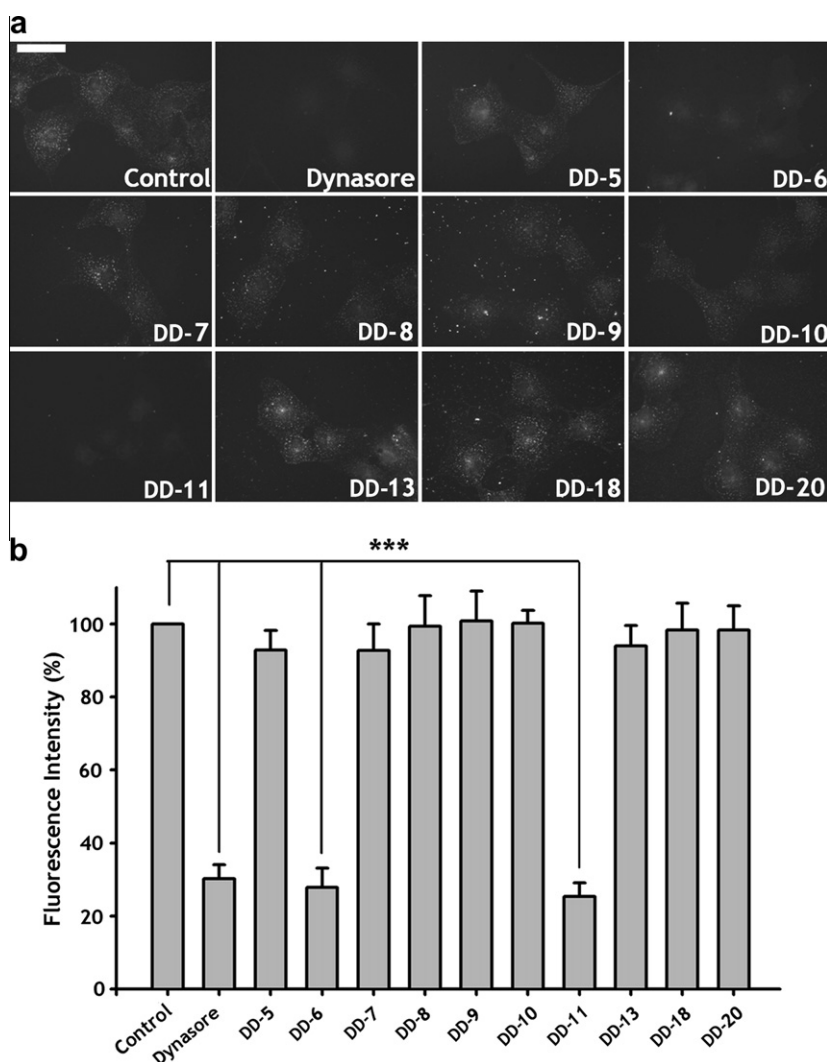


Figure 2. The effect of dynasore and derivatives on transferrin uptake. Cos-7 cells were starved for 2 h with serum free medium and treated with TexasRed conjugated transferrin for 10 min in the presence of 80 μ M synthesized compounds in 0.1% DMSO. The control experiment was done in the presence of 0.1% DMSO. (a) The fluorescence microscopic images of TexasRed–transferrin in Cos-7 cells. All images were collected with 200 ms exposures. Scale bar = 50 μ m. (b) The amount of transferrin uptake was quantified with average fluorescence intensity of internalized TexasRed–transferrin. Fluorescence intensity was normalized to the average fluorescence intensity of control. Data are means \pm s.e. (control, 100, n = 17; dynasore, 30.2084 \pm 3.8011, n = 15; DD-5, 92.8422 \pm 5.3795, n = 15; DD-6, 27.8135 \pm 5.2839, n = 13; DD-7, 92.6877 \pm 7.2998, n = 17; DD-8, 99.3377 \pm 8.3947, n = 17; DD-9, 100.8126 \pm 8.1829, n = 17; DD-10, 100.1685 \pm 3.5262, n = 15; DD-11, 25.3431 \pm 3.7935, n = 17; DD-13, 94.0383 \pm 5.5011, n = 14; DD-18, 98.2969 \pm 7.3932, n = 16; DD-20, 98.2782 \pm 6.6423, n = 15; *** P < 0.01).

amin GTPase activity in a dose-dependent manner but more potent than dynasore with IC_{50} of 5.1 μ M and 3.6 μ M, respectively, close to the IC_{50} determined in cells for the inhibition of transferrin uptake (Fig. 3d). They also inhibit the enzymatic activity of the mitochondrial Drp1, but do not affect the activity of small GTPase Cdc42 in the presence of its RhoGAP (Fig. 3e and f). It appears to be hydrogen bonding acceptor and donor group that are necessary for inhibition of dynamin GTPase. In addition, 3' position seems

to be the key region for interaction between dynamin and compounds (Table 1).

The effect of DD-6 and DD-11 on transferrin uptake is completely reversible, as after 30 min preincubation with analogues followed by removal from the medium, transferrin uptake completely returned to normal levels within 30 min (Fig. 4). The recovery was faster in DD-6 and DD-11 treated cells than dynasore treated cells (after 10 min washout, recovery is 56.5955 ± 4.7102

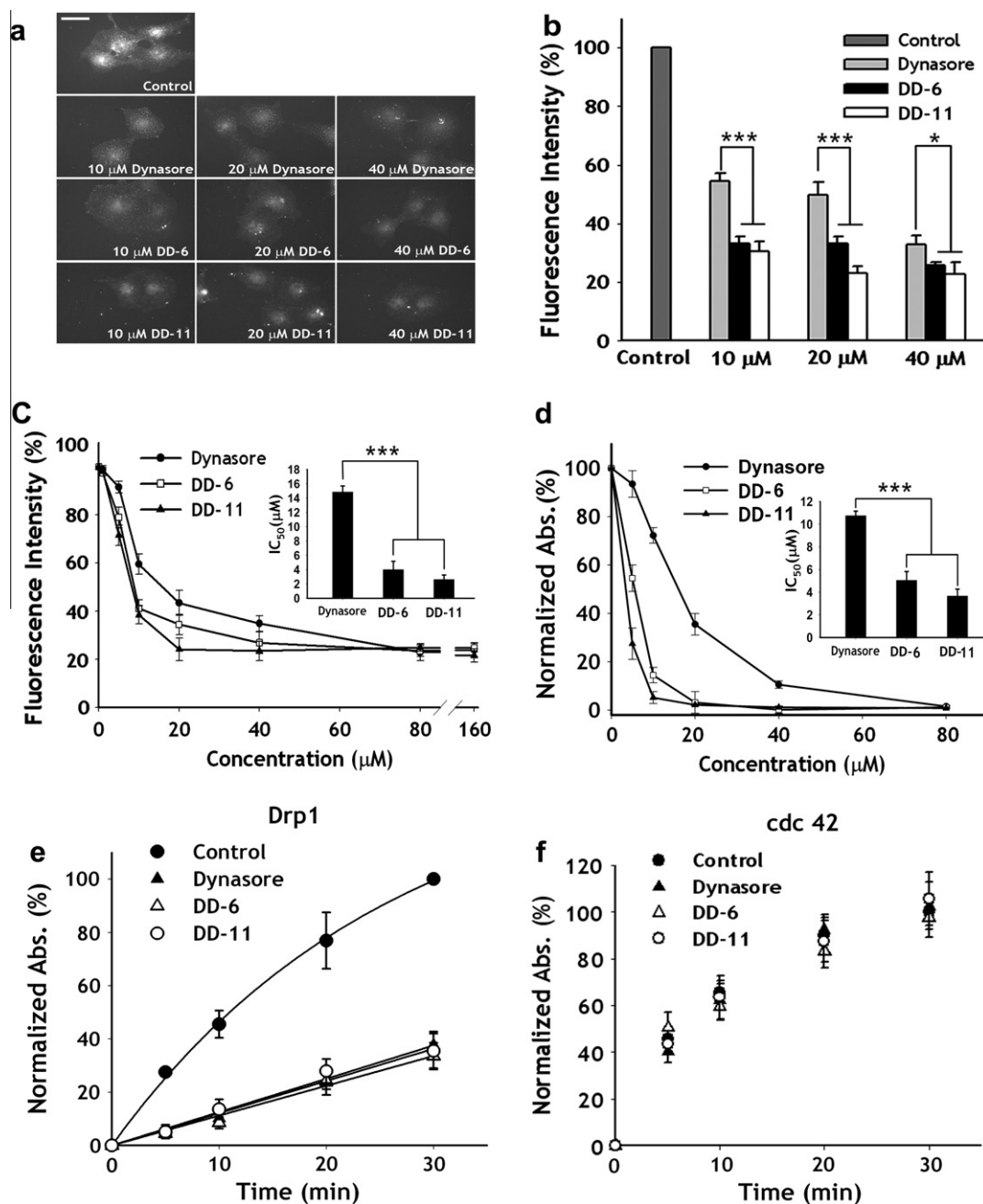


Figure 3. Determination of kinetics parameters for the effects of dynasore derivatives on transferrin uptake and GTPase activity of dynamin. Cells were incubated with TexasRed-transferrin and 10–40 μ M compounds without preincubation. The control experiment was done in the presence of 0.1% DMSO. (a) The fluorescence microscopic images of internalized TexasRed-transferrin in the presence of indicated amount of compounds. Scale bar = 50 μ M. (b) Quantification of internalized TexasRed-transferrin. Fluorescence intensity was normalized to control average fluorescence intensity. Data are means \pm s.e. (control, 100, $n = 12$; dynasore 10 μ M, 54.5726 ± 2.6233 , $n = 13$; 20 μ M, 49.6135 ± 4.6107 , $n = 11$; 40 μ M, 32.8724 ± 3.2074 , $n = 15$; DD-6 10 μ M, 33.2103 ± 2.2865 , $n = 11$; 20 μ M, 33.2103 ± 2.2865 , $n = 14$; 40 μ M, 25.8958 ± 1.0456 , $n = 13$; DD-11 10 μ M, 30.4733 ± 3.4038 , $n = 15$; 20 μ M, 22.9712 ± 2.3640 , $n = 12$; 40 μ M, 22.6976 ± 4.2634 , $n = 13$; *** $P < 0.01$, * $P < 0.1$). (c) Determination of median inhibition concentration (IC_{50}) on transferrin uptake. Inset indicates calculated IC_{50} value. (d) IC_{50} for the effects of dynasore derivatives on GTPase activity of dynamin. The GTPase activity of 1 μ M native dynamin1 was determined at low salt condition (15 mM) in the presence of indicated amount of dynasore, DD-6, and DD-11. Inset indicates IC_{50} . *** $P < 0.01$. (e) Effect of dynasore derivatives on GTPase activity of 2 μ M Drp1 in the presence of 80 μ M dynasore, 40 μ M DD-6, and 20 μ M DD-11. (f) Effect of dynasore derivatives on GTPase activity of 1 μ M Cdc42 determined in the presence of 0.5 μ M RhoGAP domain of TCGAP.

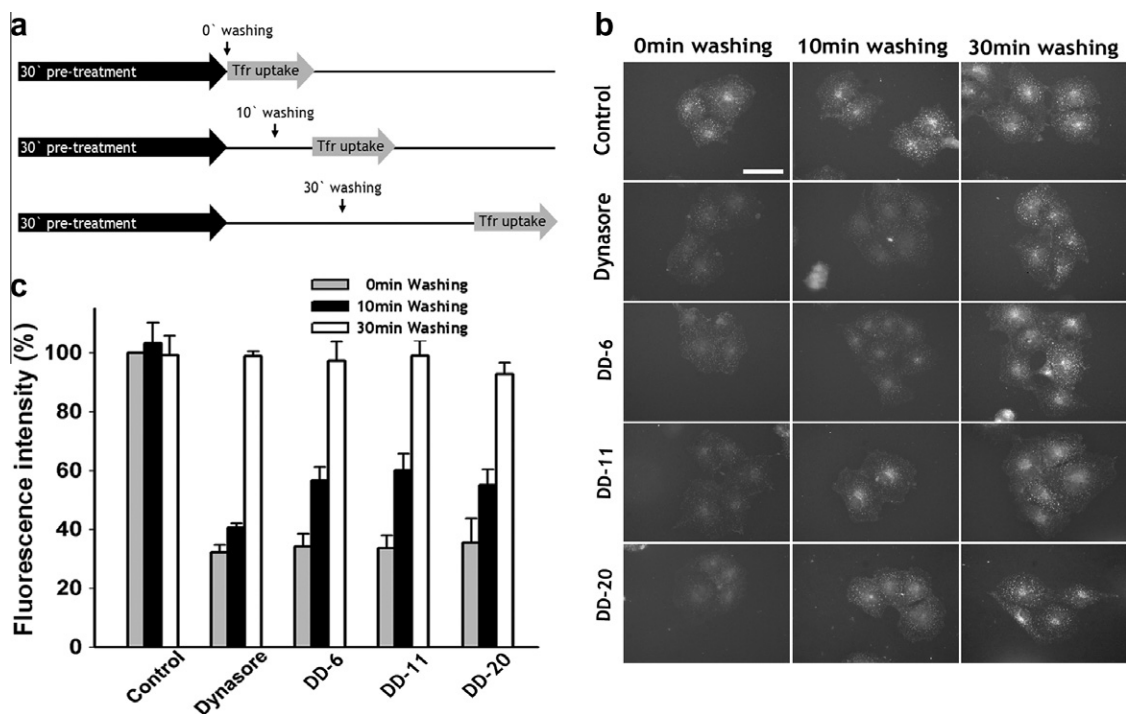


Figure 4. Reversible inhibition activity of dynasore and derivatives to endocytosis. (a) Schematic diagram of experimental strategy used for measuring the reversible activity. Cos-7 cells were pre-incubated with dynamin inhibitors (control: 0.1% DMSO, dynasore 80 μ M, DD-6 40 μ M, DD-11 20 μ M, DD-20 80 μ M) for 30 min at 37 $^{\circ}$ C, then measured the amount of transferrin uptake after washing-out for 0, 10, or 30 min. (b) TexasRed–transferrin images were collected with same exposure time (200 ms), Scale bar = 60 μ m. (c) The amount of transferrin uptake was quantified with average fluorescence intensity of internalized TexasRed–transferrin. Fluorescence intensity was normalized to the average fluorescence intensity of the control. Data are means \pm s.e. (control: 0 min, 100, $n = 14$; 10 min, 103.2277 \pm 6.9714, $n = 14$; 30 min, 99.1898 \pm 6.6613, $n = 15$; dynasore 0 min, 32.2865 \pm 2.4753, $n = 16$; 10 min, 40.5516 \pm 1.4943, $n = 15$; 30 min, 98.9139 \pm 1.5462, $n = 16$; DD-6 0 min, 34.2131 \pm 4.3470, $n = 14$; 10 min, 56.5955 \pm 4.7102, $n = 16$; 30 min, 97.3173 \pm 6.4430, $n = 16$; DD-11 0 min, 33.6497 \pm 4.3162, $n = 15$; 10 min, 60.0607 \pm 5.7320, $n = 17$; 30 min, 99.0156 \pm 5.1484, $n = 15$; DD-20 0 min, 35.4970 \pm 8.1782, $n = 14$; 10 min, 55.1139 \pm 5.2791, $n = 14$; 30 min, 92.6970 \pm 3.8849, $n = 15$).

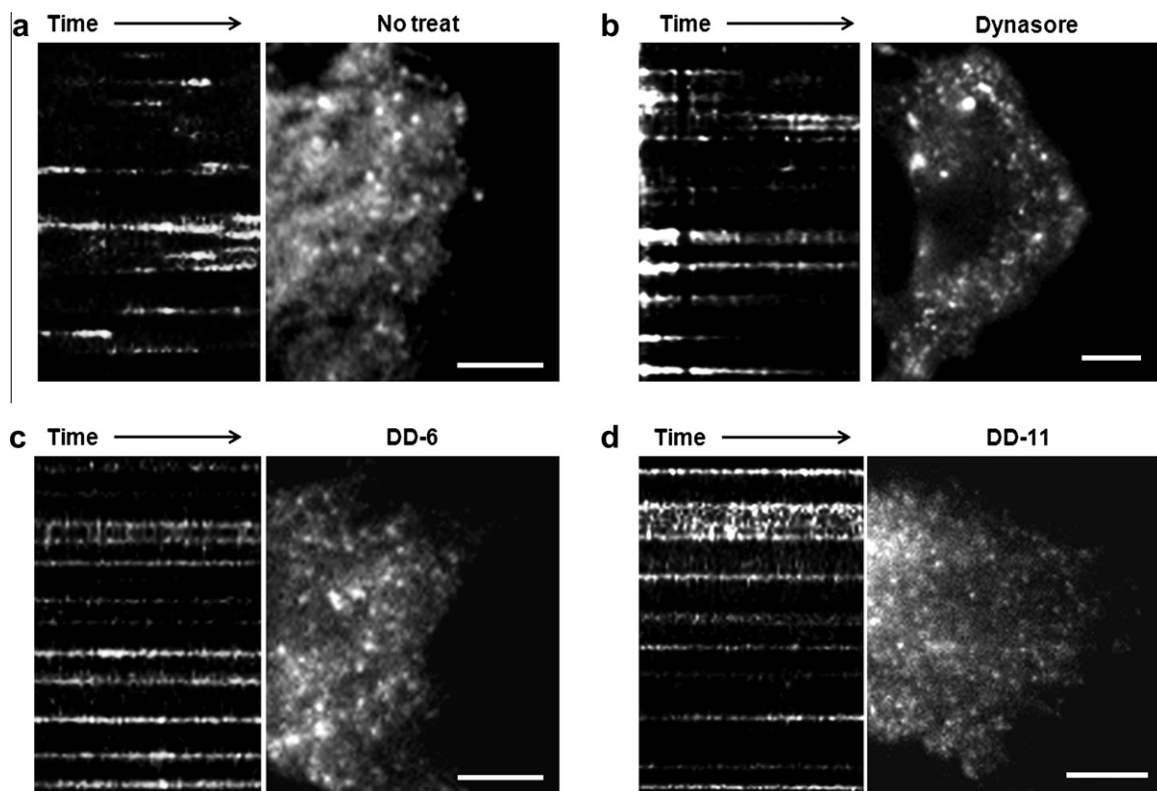


Figure 5. DD-6 and DD-11 stabilize clathrin-coated spots on the plasma membrane. TIRFM image of a COS-7 cell transiently transfected with mRFP-LCa. Time-lapse series were collected for 5 min at 37 $^{\circ}$ C in the presence or absent of dynasore, DD-6 or DD-11. Each still image corresponds to a frame acquired after 240 s and 140 s data collection, kymographs (time) represents the complete time-lapse series obtained with the line scan (100 ms exposure, acquired every 2 s).

Table 2
HPLC characterization of dynasore derivatives for purity determination

Compounds	Retention time (min)	Purity (%)
Dynasore	9.65	95.4
DD-6	8.97	93.6
DD-11	14.32	96.3

for DD-6, 60.0607 ± 5.7320 for DD-11, 40.5516 ± 1.4943 for dynasore). Interestingly, DD-20 which didn't exhibit inhibitory activity without preincubation, showed a comparable and reversible inhibition on transferrin uptake after 30 min preincubation (Fig. 4).

To study in more detail the effects of DD-6 and DD-11 compared to dynasore on the formation of clathrin-coated pits, total internal reflection microscopy (TIRFM) was performed in COS-7 cells transfected with clathrin (mRFP-LCa).²¹ TIRFM showed that mRFP-LCa is recruited to the plasma membrane in a punctate pattern which appears and disappears and have life spans ranging between 20 and 60 s (Fig. 5a). Upon incubation for 30 min with 10 μ M dynasore (which is suboptimal concentration for dynamin inhibition), some of mRFP-LCa spots become stable for long periods but many of them are still able to bud off from the membrane (Fig. 5b). In contrast, upon incubation for 30 min with 10 μ M DD-6 or DD-11, most of mRFP-LCa coats remain locked at their starting positions on the membrane, suggesting DD-6 and DD-11 block dynamin-mediated membrane fission more potently than dynasore (Fig. 5c and d).

Compared to conventional genetic or immunological tools, small chemical molecule dynamin inhibitors have the potential to study the dynamic nature of endocytic events in cells. Dynasore was discovered by chemical genetics discovery approach and has proven to be a useful tool for studying membrane traffic.^{22–26} We have designed a series of dynasore derivatives, and found that introduction of chlorine atoms or dimethyl substitution at 4' and 5' position on phenyl ring completely lost the dynasore's inhibitory effect on dynamin GTPase. In contrast, the substitution of hydroxyl group of 3-position on the naphthyl ring in dynasore to hydrogen (DD-6) and introduction of hydroxyl group at 3' and methoxy group at 4' on phenyl ring (DD-11) significantly increase inhibitory potency on dynamin GTPase (Table 2). Using TIRF microscopy, we further showed that DD-6 and DD-11 stabilize clathrin-coated spots on the plasma membrane at the concentration of 10 μ M, which is suboptimal concentration for dynasore to inhibit dynamin. They did not induce any noticeable toxicity to the cells even with 12 h incubation (Supplementary Fig. 2). Besides, DD-6 has comparable solubility in aqueous solution to that of dynasore (Supplementary Fig. 3). Although DD-11 is less soluble (Supplementary Fig. 3) but its IC_{50} for transferrin uptake is 3 times less than that of dynasore. All in all, our results display considerable promise as leads for the development of more potent analogues for dynamin inhibition.

Acknowledgments

This work was supported by Grants from the Korea Science and Engineering Foundation (R01-2006-000-10818-0) and the Brain Research Center of the 21st Century Frontier Research Program (M103KV010009-06K2201-00910) to S.C. funded by the Ministry of Education, Science and Technology, Republic of Korea. TIRF microscopy data for this study were acquired and analyzed in the Biomedical Imaging Center at Seoul National University College of Medicine.

Supplementary data

Supplementary data associated with this article can be found, in the online version, at doi:10.1016/j.bmcl.2010.06.092.

References and notes

- Abazeed, M. E.; Blanchette, J. M.; Fuller, R. S. *J. Biol. Chem.* **2005**, *280*, 4442.
- Cao, H.; Weller, S.; Orth, J. D.; Chen, J.; Huang, B.; Chen, J. L.; Stammes, M.; McNiven, M. A. *Nat. Cell Biol.* **2005**, *7*, 483.
- Damke, H.; Baba, T.; Warnock, D. E.; Schmid, S. L. *J. Cell Biol.* **1994**, *127*, 915.
- Hill, E.; van Der Kaay, J.; Downes, C. P.; Smythe, E. *J. Cell Biol.* **2001**, *152*, 309.
- Nabi, I. R.; Le, P. U. *J. Cell Biol.* **2003**, *161*, 673.
- Nichols, B. *J. Cell Sci.* **2003**, *116*, 4707.
- Roux, A.; Uyhazi, K.; Frost, A.; De Camilli, P. *Nature* **2006**, *441*, 528.
- Hill, T.; Odell, L. R.; Edwards, J. K.; Graham, M. E.; McGeachie, A. B.; Rusak, J.; Quan, A.; Abagyan, R.; Scott, J. L.; Robinson, P. J.; McCluskey, A. *J. Med. Chem.* **2005**, *48*, 7781.
- Hill, T. A.; Gordon, C. P.; McGeachie, A. B.; Venn-Brown, B.; Odell, L. R.; Chau, N.; Quan, A.; Mariana, A.; Sakoff, J. A.; Chircop, M.; Robinson, P. J.; McCluskey, A. *J. Med. Chem.* **2009**, *52*, 3762.
- Hill, T. A.; Odell, L. R.; Quan, A.; Abagyan, R.; Ferguson, G.; Robinson, P. J.; McCluskey, A. *Bioorg. Med. Chem. Lett.* **2004**, *14*, 3275.
- Odell, L. R.; Chau, N.; Mariana, A.; Graham, M. E.; Robinson, P. J.; McCluskey, A. *ChemMedChem* **2009**, *4*, 1182.
- Quan, A.; McGeachie, A. B.; Keating, D. J.; van Dam, E. M.; Rusak, J.; Chau, N.; Malladi, C. S.; Chen, C.; McCluskey, A.; Cousin, M. A.; Robinson, P. J. *Mol. Pharmacol.* **2007**, *72*, 1425.
- Macia, E.; Ehrlich, M.; Massol, R.; Boucrot, E.; Brunner, C.; Kirchhausen, T. *Dev. Cell* **2006**, *10*, 839.
- Kirchhausen, T.; Macia, E.; Pelish, H. E. *Methods Enzymol.* **2008**, *438*, 77.
- A mixture of 2-naphthohydrazide or 3-hydroxy-2-naphthohydrazide (0.5 mmol), appropriate benzaldehyde (0.5 mmol) and ceric ammonium nitrate (0.1 mmol) in 50 mL of anhydrous ethanol was refluxed at 65 °C for 3 h. The solvent was removed under reduced pressure, and the residue was partitioned between saturated sodium bicarbonate (100 mL) and $CHCl_3$ (3×30 mL). The organic layer was dried on Na_2SO_4 and evaporated under vacuum, and the residue was purified by silica gel column chromatography ($CHCl_3/MeOH$, 20:1) to afford the product as solid (DD-4–11).
- To the 2-naphthoic acid or 3-hydroxy-2-naphthoic acid (0.5 mmol) in 50 mL of absolute dichloromethane was added 4-dimethylaminopyridine (0.05 mmol), EDCI (0.6 mmol) and corresponding 2-(substituted phenyl) ethyl amine (0.5 mmol). The mixture was stirred at room temperature for 1 h and the solvent was removed under reduced pressure. The residue was partitioned between saturated sodium bicarbonate (100 mL) and $CHCl_3$ (3×30 mL). The organic layer was dried on Na_2SO_4 and evaporated under vacuum, and the residue was purified by silica gel column chromatography ($CHCl_3/MeOH$, 20:1) to afford the product as solid (DD-12–19).
- All starting materials were purchased from Aldrich (St. Louis, MO, USA) and TCI (Tokyo, Japan). Proton nuclear magnetic resonance spectroscopy was performed on a JEOL JNM-LA 300WB spectrometer, and spectra were taken in $CDCl_3$ or $DMSO-d_6$. Unless otherwise noted, chemical shifts are expressed as ppm downfield from internal tetramethylsilane, or relative ppm from NMR solvent. Data are reported as follows: chemical shift, multiplicity (s, singlet; d, doublet; t, triplet; m, multiplet; b, broad; app., apparent), coupling constants, and integration. Mass spectroscopy was carried out on MALDI-TOF and LC-MS instruments.
- For dynamin inhibition efficiency test of dynasore and derivatives, starved cells were incubated in Dulbecco's PBS (DPBS) containing 20 μ g/ml Texas red transferrin (Invitrogen, Eugene, OR) and various concentration (10–80 μ M) dynasore and derivatives for 10 min at 37 °C with or without preincubation. Cells were washed with cold DPBS three times and removed surface binding Texas red transferrin in acid stripping solution (150 mM NaCl, 2 mM $CaCl_2$ and 25 mM CH_3COONa , pH 4.5) and fixed in 4% paraformaldehyde. To study the reversible effect of these molecules in transferrin uptake, cells were preincubated with dynasore and derivatives (80 μ M for dynasore, DD-20 and DD-13; 40 μ M for DD-6, 20 μ M for DD-11) for 30 min at 37 °C and washed with DPBS for various 0 min, 10 min, 30 min. After washing the cells, 20 μ g/ml Texas red transferrin was treated to these cells and incubated for 10 min at 37 °C.
- Images were obtained with an Olympus IX-71 inverted microscope (Olympus Optical, Tokyo, Japan) with a 40 \times , 1.0 N.A. oil lens using a CoolSNAP-Hq CCD camera (Roper Scientific, Tucson, AZ) driven by MetaMorph imaging software (Universal Imaging Corporation, West Chester, PA) with a Texas red optimized filter set (Omega Optical, Brattleboro, VT). Light from a mercury lamp was shuttered using a VMM1 Uniblitz shutter (Vincent Associates, Rochester, NY). Analysis and quantification of data were performed using MetaMorph software and SigmaPlot 8.0 (Systat Software, Point Richmond, CA), and data were presented as mean \pm SE.
- Native dynamin I purified from mouse brain. Briefly, Amphiphysin I-SH3-GST immobilized agarose bead incubated with brain lysate for 2 h and eluted only dynamin I from Amphiphysin I-SH3-GST using high salt elution buffer (1.2 M NaCl, 20 mM PIPES, 1 mM DTT, pH 6.5). The eluted dynamin I protein was placed in a diluting buffer (30 mM Tris/HCl, 100 mM NaCl, pH 7.4) and quantified by SDS-PAGE. Human Drp1 and SNX26 RhoGAP domain were subcloned in-frame into pGEX-4T-1 vector (GE Biosciences, Piscataway, NJ) and transformed into *Escherichia coli* BL-21 and the cells were cultured in 2X-YT medium supplemented with ampicillin. After overnight induction with 0.5 mM IPTG at 25 °C, the cells were sonicated in lysis buffer (1% Triton X-100, 0.5% sodium deoxy-cholate, 20 mM Tris, pH 8.0, 150 mM NaCl, 1 mM $MgCl_2$,

1 mM EGTA, 0.1 mM PMSF). The sonicates were centrifuged for 15 min at 12,000 rpm, and the resulting supernatants incubated with glutathione–Agarose–4B beads (GE Biosciences, Piscataway, NJ) at 4 °C for 30 min. After incubation, slurries were incubated with 30 mM GSH for 1 hr at 4 °C and corrected supernatants followed by dialysis by assay buffer. GTPase activity was measured by using the GTPase Enzyme Linked Inorganic Phosphate Assay (cytoskeleton). Briefly, 1 μM dynamin I mixed with indicated concentration of dynasore and derivative DD-6, DD-11. These protein mixtures were added to Enzyme Linked Inorganic Phosphate Assay (ELIPA) mixture and incubated with 25 μl of 10 mM GTP for 1 h at 37 °C. To measure the released phosphate amount by GTP hydrolysis, we used monochromatic spectrophotometer PowerWave XS (BioTek instruments, Winooski, VT) and checked absorbance at 360 nm wave length. The absorbance was normalized to maximum and minimum absorbance value of each compound and analyzed IC₅₀ by nonlinear regression curve fitting using Graphad Prism 5 software. GTPase activity of 1 μM Drp1 was measured by same method with dynamin I GTPase activity. To identify the effect of dynasore derivatives to Cdc42 GTPase activity, 1 μM Cdc42 (Cytoskeleton) was mixed with 0.5 mM GST tagged human SNX26 RhoGAP domain, and added to prepared ELIPA mixture with 1 mM GTP. The amount of inorganic phosphate released by GTPase activity was measured by using the GTPase Enzyme Linked Inorganic Phosphate Assay in the presence of 0.5 μM GST tagged human TCGAP RhoGAP domain. The amount of inorganic

phosphate released by Cdc42 in the presence of 0.1% DMSO (control), 80 μM dynasore, DD-6 or DD-11 was measured at 360 nm and plotted as a function of time.

21. For total internal reflection fluorescence (TIRF) microscopy, cells were imaged using an Olympus IX-71 microscope fitted with a 60× 1.45 N.A and 100× 1.45 N.A. TIRF lens and controlled by CellTM software (Olympus). Laser lines (488 and 561 nm diode lasers) were coupled to the TIRFM condenser through two independent optical fibers. The calculated evanescent depth was ≈150 nm. Cells were typically imaged in two channels by sequential excitation with 0.15 s exposures and detected with back-illuminated Andor iXon887 EMCCD camera (512 × 512, 16-bit; Andor Technologies). Image J program (National Institutes of Health) was used for analysis.
22. de Beco, S.; Gueudry, C.; Amblard, F.; Coscoy, S. *Proc. Natl. Acad. Sci. U.S.A.* **2009**, *106*, 7010.
23. Lu, W.; Ma, H.; Sheng, Z. H.; Mochida, S. *J. Biol. Chem.* **2009**, *284*, 1930.
24. Miyachi, K.; Kim, Y.; Latinovic, O.; Morozov, V.; Melikyan, G. *B. Cell* **2009**, *137*, 433.
25. Newton, A. J.; Kirchhausen, T.; Murthy, V. N. *Proc. Natl. Acad. Sci. U.S.A.* **2006**, *103*, 17955.
26. Otsuka, A.; Abe, T.; Watanabe, M.; Yagisawa, H.; Takei, K.; Yamada, H. *Biochem. Biophys. Res. Commun.* **2009**, *378*, 478.